Intermolecular magnetic interactions in stacked DNA base pairs

Fernando A. Martínez and Gustavo A. Aucar

Received Xth XXXXXXXXXX 201X, Accepted Xth XXXXXXXXX 201X
First published on the web Xth XXXXXXXXXX 201X
DOI: 10.1039/b000000x

The influence of pi-stacking on magnetic properties of atoms that belongs to adenine-thymine and guanine-cytosine pairs in sequences of three and five layers of DNA base pairs was analysed. As probes we used NMR spectroscopic parameters, which are among the most useful tools to learn about the transmission of magnetic interactions in molecules. Four DFT functionals were employed: B3LYP, BHANDLYP, KT2 and KT3, together with the SOPPA method. Besides, given that the number of non-hydrogen atoms of the supramolecular systems studied here is larger than 50 we applied a locally dense basis set scheme. Our results show that the piling up of few Watson-Crick base pairs above and below of a given pair, modify its NMR spectroscopic parameters in an amount that may be measurable and the percentage of variation does not depend on dispersion. We found that magnetic shieldings are more sensitive than the J-couplings, and also that some atoms are more sensitive than others. Stacking do affect the shielding of non-hydrogen atoms like nitrogens, that are donors in hydrogen bonds, HB, and the carbons bonded to them. The amount of variation of those shieldings was found to be among 2% to 5% when the pairs are considered first as isolated, and then, placed in the middle of a sequence of three layers of base pairs. Such a variation become vanishingly small when the sequence contain more than three layers, showing that the stacking effect on NMR spectroscopic parameters has a local nature. We have also found a pattern for shieldings. First, equivalent atoms of similar monomers (thymine and adenine, or guanine and cytosine) do have similar values of absolute shieldings in isolated pairs, and the amount of its variation from isolated to aggregates of few pairs is also similar, meaning that equivalent atoms are affected in a similar manner by the pi-stacking. Second, the hydrogen atoms which belongs to hydrogen bonds are more sensitive to the piling up than the non-hydrogen atoms.

1 Introduction

Main DNA electronic interactions act through the hydrogen bonds, HB, along the plane of the base pairs, or perpendicular to it, through stacking interactions. These last molecular interactions can be related with π - π stacking interactions and also the so called "diagonal interactions". Are all the mentioned interactions equally important? Rezáč and Hobza have shown that H-bonding contributes less to the stability of DNA than stacking.[1]

Several studies were conducted to learn more about any of the three interactions. There were some studies on the strength of the HB, oriented to stablish the origin of the enhanced stability of the HB in adenine-thymine (AT) DNA base pairs,[2] the functionality of the twist-angle on the stability of the DNA structure,[3] the estimation of the individual contributions of each intermolecular HB, in AT and cytosine-guanine, CG, base pairs[4] and the role of the dispersion energy and electrostatic energy on the geometry and stability of the B-DNA helix.[5]

In a work about the importance of the charge transfer and the resonance-assisted hydrogen bond, RAHB, on the stabilization of Watson-Crick DNA base pairs, Fonseca and coauthors have found that the electrostatic interactions and charge transfer are of similar importance, and that indeed the π electrons provide an additional stabilizing component.[6] They found that it is the charge transfer nature of the HB, rather than the RAHB, that, together with the classical electrostatic interaction is vital to the behavior and the stability of DNA.

On the other side, stacking or interbase interactions were recently studied to get a deeper understanding of the stacking forces necessary to break fragments of DNA base-pairs while leaving hydrogen bonds intact, at the level of individual pairs. These studies are of great interest due to its applied use; for example, to make more informed decisions in the design of dynamic DNA-based nanoscale devices.[7]

The stacking force may be related with the π-π stacking interactions[8] and the so-called "diagonal interactions", cross terms, that appears among a base in one base pair and the opposite base in the next base pair.[3] These cross terms were found to be more important for GC-rich sequences than for the equivalent AT-rich sequences.

Most of the above mentioned studies are related with electronic energies, charge distributions and electric properties. To our knowledge there are no equivalent studies of magnetic properties. On these grounds we decided to search about whether the pi-stacking interactions can influence the NMR spectroscopic parameters in a way that could be measurable. One of the aims of

* Corresponding author: gaaucar@conicet.gov.ar
Instituto de Modelado e Innovación Tecnológica, CONICET, and Departamento de Física - Facultad de Ciencias Exactas y Naturales, UNNE, (Avda Libertad 5460, W3404AAS), Corrientes, Argentina

this work is to show the likely influence of piling up base-pairs (til five base-pairs) on the magnetic properties of a given pair, together with the appearance of cooperativity effects in addition to that of stacking and HB effects. Furthermore another aim of this work is to shed some light on whether there are some particular atoms belonging to the selected base-pairs that may be more sensitive to the presence of other base-pairs in the helical layers of fragments of DNA.

During the last few decades there was an increasing interest in the studies of structure and dynamics of DNA molecules using different techniques. NMR is one of the most powerful and widespread used. Nearly half of all current RNA structures were determined by using NMR techniques.[9] Not only the structure but also the electronic mechanisms that underlies the NMR spectroscopic parameters were and are of interest. The seminal work of Juranic and co-workers on the transmission of J-couplings through HB in nucleic acid bases opened the door to new applications of NMR on DNA molecules. They have shown experimentally that J-couplings are transmitted through HB and are sensitive to extended environments containing HBs, and also that there are intramolecular and intermolecular J-couplings in proteins.[10,11]

Turning to the computational side of the NMR spectroscopic parameters of Watson-Crick DNA, Marek and co-authors have found theoretical results that are close to experimental values in isomers of adenine using density functional theory, DFT.[12] Similar comparative studies were performed by Fiala and coauthors on quaternary carbons in RNA molecules.[13] There were further studies showing that theoretical chemical shifts are valuable for the characterization of nucleic acid conformation.[14] The sensitivity of the spin-spin couplings to base pairing as well as the agreement with the experiments depend strongly on the type of nuclei involved and the number of bonds separating them.[13] They can be used to gain some insights into the nature of HB.[15,16]

Furthermore, the inclusion of intermolecular interactions on the calculations of ^{15}N chemical shifts give results that are in better agreement with experimental values.[17] The NMR spectroscopic parameters can also give information about the HB donor-acceptor distances in nucleic acids.[16]

Concerning cooperativity effects it was shown that they can appear due to HB in H-bonded nucleobases when they are taken as dimers[18], or when monomers are extended in planar configurations;[19] but it is not still clear whether such effects can also be transmitted through the helical arrangements of nucleic acids.

In our group of research we have obtained some understanding about the electronic mechanisms that are involved in the magnetic perturbations transmitted through HBs. We have shown that J-couplings and shieldings of H-bonded systems are influenced by its geometry and degree of covalency, as well as the intra- and intermolecular resonance, not only for RAHB systems.[20] Besides, studying malonaldehyde and few of its derivatives we have found which are the electronic mechanisms that indicate when a system has a RAHB.[21] We also found cooperativity effects on magnetic properties of linear chains, $(CNH)_n$ and $(NCH)_n$ at DFT/B3LYP[22,23] and SOPPA[24–26] levels of approach.[27] Furthermore we have also found that there are long-range electronic effects (transmitted through few nanometers) that can give measurable values of J-couplings in unsaturated systems.[28]

In this work we address the following questions: i) Are the NMR spectroscopic parameters good enough to describe the influence of the piling up of Watson-Crick base pairs on a base pair of a giving layer?, ii) Being the main forces involved in the stability of helical DNA originated in the hydrogen-bonds and pi-stacking, how large are their influences on those spectroscopic parameters?, iii) Which are the most sensitive atoms or molecular regions of each base pair? and iv) How sensitive is each one of both (σ and J-coupling) NMR spectroscopic parameters to the just mentioned piling up?

We used some well-known DFT functionals and *ab initio* methods to calculate the NMR spectroscopic parameters. The functionals B3LYP, BHANDLYP[29], and KT2[30] and KT3[31] were validated with the results of second-order polarization propagator approach, SOPPA in monomers of thymine. Accurate calculations at SOPPA level can only be performed for such monomers using large enough basis sets.

In the first part of this article we analize how good are the results of calculations of NMR spectroscopic parameters performed with the DFT functionals mentioned above. Then we show our analysis of those parameters for AT and GC pairs, isolated from a sequence of a DNA molecule, and being part of three to five stacked base pairs. The last section is devoted to highlight our main conclusions.

2 Models and Procedures

As mentioned above, our main concern is focused on the analysis of the influence of both, HB and the presence of vicinal layers of DNA base pairs, on the NMR spectroscopic parameters of a given pair located in the middle of them. Our calculations were seized by some well known restrictions that one should allways consider, like the largest size of the molecules that can be studied with enough accuracy. So we performed SOPPA calculations for monomers, and compared them with that of selected

DFT schemes which better describe the magnetic properties we are interested in.

At this stage solvent effects shall not be considered though they will be included in the next future. We are interested first to quantify the effects of the presence of layers of base pairs alone, up and down of a given pair.

The helical layers were taken from the Protein Data Bank (**PDB ID**: 1BNA). Few layers of a double-stranded B-DNA dodecamer were selected to use them as our first trial of this kind of studies. Its crystal structure has the following sequence of nucleotides: 5' d(CGCGAATTCGCG) 3'. In order to make its treatment feasible we take out all sugars and phosphate groups, and replaced them by hydrogen atoms. The geometrical structure of each layer was not modified, meaning that experimental geometries of all layers of base pairs are taken as they are when sugars and phosphate groups are included. So, the NMR spectroscopic parameters will not be dependent on the replacement of lateral groups by hydrogens.

Given the different number of HBs that are stablished among purine and pyrimidine base pairs we selected two types of sequences: one that is richer in guanine-cytosine (GC) bases and another one that is richer in adenine-thymine (AT) bases. As an example, for layers that have more GC pairs we selected two sequences with an odd number of basis: one, three and five base pairs which have the same central pair.

We built the structures considering the sequence of the base pairs taken from the PDB code, from which the sequence of the complementary strand is easily obtained. So, in order to clearly show how the pairs do appear in the layers, we give the following scheme:

Base pair	1	2	3	4	5	6	7	8	9	10	11	12
Main strand	**C**	**G**	**C**	**G**	**A**	**A**	**T**	**T**	**C**	**G**	**C**	**G**
Complementary strand	G	C	G	C	T	T	A	A	G	C	G	C

So the following sequence was fixed: GCG (following the main strand or following the numeration of the pairs corresponding to 234) and CGCGA (following the pair numbers 12345). They were chosen in such a way that they share the same central base pair, which in this case is the one numbered as 3.

For layers that are richer in AT pairs are built from the ATT sequences (which correspond to 678) and AATTC sequences (which correspond to 56789). The central pair, the number 7, is the same in both sequences.

We also analysed the NMR spectroscopic parameters on isolated monomers and dimers. Their geometries were taken as such from the PDB code, or were theoretically optimized at B3LYP/cc-pVTZ level of theory. This was applied to each monomer, *i.e.* guanine, cytosine, adenine and thymine, and also to the GC and AT pairs. The analysis of those pairs was performed in order to learn more about the influence of the HB bonding on the NMR parameters of each monomer, and also about how important is the influence of the piling up of dimers that are located up and down of the the base pair of interest.

Our procedure is such that we can distinguish the geometric effects to the electronic effects on the NMR spectroscopic parameters of the base pairs.

3 Levels of Theory and Computational Details

The polarization propagator at its second-order of approach, SOPPA, is one of the most accurate available methods to calculate magnetic molecular properties, asuming that large enough basis sets are used.[24–26,32]

One must include electron correlation, specially for magnetic shieldings of ^{15}N, in order to obtain accurate shielding tensors in molecules with multiple bonds.[33] This is also important for shieldings and J-couplings of carbons involved in multiple bonded carbons, specially when they are bonded to nitrogen or oxygen atoms.[34–36] In our case the number of atoms that belongs to any of our base pairs is larger than the maximum number of them that one can consider if wants to make accurate calculations at SOPPA level. This is even worst for calculations at coupled-cluster level of theory. It is known that calculations at SOPPA level are less expensive than the coupled-cluster and becomes a good alternative for large systems.[32,37,38]

So, in the case of monomers we calculated the NMR spectroscopic parameters at SOPPA level of approach. In all other cases we used DFT, with the constraint that the choice of the exchange-correlation functional is critical for calculations of magnetic shieldings in H-bonded systems; even though this is not so in all cases.[39]

Besides we reduced the computational efforts by applying the locally dense basis set, LDBS, scheme.[40–42] This scheme is such that one can describe magnetic properties of different portions of a molecule with different accuracy. One is then able to get accurate results with much smaller computational costs as compared with the usual scheme of including the same basis set to each atom of the whole molecule.

We started the evaluation of the performance of different DFT functionals and basis sets on our selected bases by performing calculations of shieldings and J-couplings in thymine. The SOPPA approach was only applied to calculate the NMR shielding of the nitrogen and hydrogen atoms that belongs to the HB among adenine and thymine (see atoms N_3 and H_3 in Fig. 1 (a)). In this case we performed a serie of calculations with Gaussian[43,44] and Dunnings[45–48] basis sets.

The single-origin gauge scheme was applied in all SOPPA calculations and the gauge origin was placed

at the site of the atom of interest. The DFT calculations were performed employing both, gauge-including atomic orbitals and London orbitals, to guarantee the origin-independence of our results.[49–51] Concerning the selected basis sets, we used both, Pople-type basis sets (6-31G[43], 6-311G(2df,2pd)[44]) and the standard correlated-consistent basis sets of Dunning and collaborators: the polarized valence basis sets: cc-pVXZ (X = T, Q)[45,46], their augmented extensions: aug-cc-pVXZ (X = T, Q)[47] and their improved basis sets: cc-pCVXZ and aug-cc-pCVXZ (X = T, Q).[48]

Optimization of the selected molecular geometries were performed at DFT/B3LYP/cc-pVTZ level of theory, using the DALTON2016 code.[52] All geometries and selected values of NMR spectroscopic parameters calculated at different level of theory with different basis sets are given as Supporting Information.

4 Results and Discussion

The systems we are interested in are medium-size molecular systems, which contain between 19 and 95 non hydrogen atoms. We start this Section showing results of calculations of NMR spectroscopic parameters of monomers of thymine. In this case we were able to compare DFT with SOPPA results in order to select which functional would be the best to use, together with the optimum basis sets. Then we show the optimal LDBS scheme.

Afterwards, results of calculations for isolated AT and GC pairs, few layers of DNA base pairs together with its analysis will be given following the model exposed in Section 2.

4.1 NMR Spectroscopic Parameters of Thymine and Adenine

The dependence of SOPPA results with the quality of basis sets is well known,[53] though it seems to be more important in our molecules than in other molecular systems. In Table 1 we show that SOPPA values for the shielding of N_3 and H_3 of the molecule of thymine become smaller when the size of the basis set grows up. For $\sigma(N_3)$ the calculations with cc-pVTZ and aug-cc-pCVTZ basis sets give results whose difference is close to 40 ppm. A similar behavior is observed for $\sigma(H_3)$, whose variation is close to 60%.

Table 1 also shows that one needs to describe with higher accuracy than usual the core of atoms in our monomers. When the non-hydrogen atoms are described either with cc-pVTZ or cc-pCVTZ, the value of $\sigma(N_3)$ changes 34 ppm. This behavior is similar to that obtained when augmented basis sets are employed.

Table 1 Magnetic shieldings of N_3 and H_3 in thymine, calculated at SOPPA level of approach with different basis sets. All values are given in ppm

	cc-pVTZ	aug-cc-pVTZ	cc-pVQZ	cc-pCVTZ	aug-cc-pCVTZ
σ_{N3}	138.69	128.66	106.16	104.77	96.28
σ_{H3}	60.02	52.14	33.91		23.13

The following four DFT functionals were selected to compare their results with that of SOPPA: B3LYP[22,23], BHANDHLYP[29], KT2[30] and KT3[31]. As usual we had to make a compromise among accuracy and feasibility.

We first analized the performance of each of those functionals with a different basis sets on thymine. In these calculations the same basis set was used for all atoms. Its results are given in Table 2. After these findings we were able to select the best basis set we could use on our larger systems.

The main differences appear for non-hydrogen atoms. In the case of B3LYP, the values of $\sigma(N_3)$ falls down when better basis sets are used. The same behavior is observed for $\sigma(H_3)$. For C_2 its shielding becomes less diamagnetic (around 15%) when the basis set changes from cc-pVTZ to cc-pCVTZ. In the case of $\sigma(C_2)$ the variation is $\simeq$ 30%, being similar to what happens when the basis set goes from cc-pVTZ to cc-pVQZ. At the end, $\sigma(C_4)$ varies from 17.16 ppm to 11.47 ppm when the basis set is changed from cc-pVTZ to aug-cc-pCVTZ.

From the previous analysis of shieldings on thymine, it appears that, for the set of atoms studied (we consider that they represent the behavior of all others in thymine) the usual cc-pVTZ basis set is not good enough. Then, one should use at least the cc-pCVTZ basis set.

For J-couplings the performance of B3LYP with such a basis set is is such that it is a good choice, as observed in Table 3. They give results close to that of SOPPA. It also appears that J(N_3-H_3) is almost saturated for aug-cc-pVQZ basis set (-85.92 Hz) or equivalently for cc-pCVTZ (-85.85 Hz). In the case of J(C_4-N_3) = -9.31 Hz at SOPPA/aug-cc-pCVTZ level of approach this is close to that given in Table 3.

On the other hand, the behavior of the results obtained with the functional BHANDHLYP, as happens also with the KT2 and KT3 functionals, is similar to that of B3LYP, but the time consumption of calculations with KT2 and KT3 is much smaller (close to 40% smaller).

The next step was to find the best LDBS scheme that optimize computational efforts.[40–42] We divided each base pair in two regions: one described with one of the best basis sets found previously and the other with smaller basis sets. The selected functional was the KT3 and the following LDBS: cc-pCVTZ for all atoms in the region more accurately described, and for atoms of carbon and nitrogen in the other region: cc-pVTZ, and 6-31G for

Table 2 Calculations of σ (in ppm) and J-couplings (in Hz) for thymine employing different DFT functionals and basis sets. Results of calculations applying the selected LDBS scheme are given between parentheses

	Functional	$\sigma(N_3)$	$\sigma(H_3)$	$\sigma(C_2)$	$\sigma(C_4)$	$J(N_3\text{-}H_3)$
cc-pVTZ	B3LYP	82.34	24.77	30.92	17.16	-83.48
	BHANDHLYP	92.47	24.68	30.80	17.18	-90.17
	KT2	93.77	24.71	48.48	36.55	-78.62
	KT3	94.58	24.86	49.02	36.96	-81.47
aug-cc-pVTZ	B3LYP	81.24 (81.17)	24.45 (24.44)	30.58 (30.49)	16.52 (16.65)	-91.75 (-91.33)
	BHANDHLYP	(91.26)	(24.38)	(30.71)	(16.75)	(-98.02)
	KT2	93.33 (93.25)	24.37 (24.35)	48.54 (48.36)	36.29 (36.35)	-87.10 (-86.56)
	KT3	93.94 (93.83)	24.54 (24.51)	49.08 (48.87)	36.83 (36.83)	-90.35 (-89.78)
cc-pVQZ	B3LYP	76.59 (76.94)	24.46 (24.49)	25.35 (25.53)	11.21 (11.36)	-87.11 (-87.19)
	BHANDHLYP	(87.65)	(24.43)	(26.46)	(12.30)	(-94.80)
	KT2	89.79 (90.20)	24.39 (24.41)	44.68 (44.89)	32.45 (32.62)	-83.73 (-83.79)
	KT3	90.48 (90.83)	24.56 (24.58)	45.39 (45.54)	33.19 (33.25)	-87.36 (-87.40)
aug-cc-pVQZ	B3LYP	75.88 (76.03)	24.35 (24.36)	25.12 (25.05)	10.56 (10.78)	-85.92 (-86.27)
	BHANDHLYP	(86.76)	(24.29)	(26.10)	(11.82)	(-93.94)
	KT2	89.04 (89.23)	24.27 (24.27)	44.03 (44.31)	31.75 (31.94)	-84.42 (-84.11)
	KT3	89.58 (89.75)	24.44 (24.44)	44.61 (44.93)	32.27 (32.53)	-87.99 (-87.70)
cc-pCVTZ	B3LYP	78.79 (78.76)	24.79 (24.79)	26.64 (26.63)	12.39 (12.38)	-85.85 (-85.79)
	BHANDHLYP	(89.90)	(24.69)	(27.73)	(13.62)	(-92.32)
	KT2	88.32 (88.26)	24.73 (24.73)	42.03 (42.03)	29.50 (29.50)	-92.72 (-92.65)
	KT3	88.81 (88.74)	24.89 (24.88)	42.35 (42.35)	29.75 (29.75)	-93.83 (-93.76)
aug-cc-pCVTZ	B3LYP	77.28 (77.23)	24.47 (24.46)	25.73 (25.71)	11.47 (11.52)	-85.90 (-85.37)
	BHANDHLYP	(88.38)	(24.40)	(27.04)	(12.85)	(-91.73)
	KT2	86.80 (86.75)	24.39 (24.38)	41.14 (41.10)	28.61 (28.65)	-92.68 (-92.15)
	KT3	87.31 (87.24)	24.55 (24.54)	41.46 (41.41)	28.90 (28.92)	-93.70 (-93.20)
cc-pCVQZ	B3LYP	74.78 (75.08)	24.58 (24.61)	23.12 (23.17)	8.79 (8.82)	-85.57 (-85.47)
	BHANDHLYP	(86.37)	(24.52)	(24.55)	(10.17)	(-92.39)
	KT2	85.24 (85.57)	24.49 (24.52)	39.65 (39.69)	27.09 (27.12)	-85.97 (-85.85)
	KT3	85.70 (85.97)	24.67 (24.69)	39.99 (40.03)	27.40 (27.41)	-88.99 (-88.85)
aug-cc-pCVQZ	KT2	84.64 (84.62)	24.33 (24.35)	39.34 (39.30)	26.74 (26.75)	-85.92 (-85.79)
	KT3	84.97 (85.00)	24.49 (24.51)	39.67 (39.64)	27.06 (27.04)	-89.02 (-88.89)

Table 3 Results of J-coupling calculations in thymine using DFT/B3LYP/KT3 and SOPPA level of theory with the cc-pVTZ basis set. All values are in Hz

	$C_4\text{-}N_3$	$N_3\text{-}H_3$	$C_2\text{-}N_1$	$N_1\text{-}H_1$
B3LYP	-8.11	-83.48	-20.21	-89.50
KT3	1.73	-81.47	-9.33	-88.72
SOPPA	-8.89	-83.73	-20.59	-88.98

hydrogens in this last region. This is shown in Fig. 1. Results of calculations with this LDBS scheme are given between parentheses in Table 2. A large reduction of time consumption was found by using this LDBS scheme together with the KT3 functional.

Even though we were interested in the effect of piling up, meaning the variation of NMR spectroscopic parameters due to stacking, in Table 4 we show how well our results do compare with previous theoretical and experimental values, that were taken from the works of Marek and his team,[12] and Hu and collaborators.[17] The chemical shift was calculated as usual:

$$\delta_X = \frac{\sigma_X^{ref} - \sigma_X^{calc}}{1 - \sigma_X^{ref}} \approx \sigma_X^{ref} - \sigma_X^{calc} \qquad (1)$$

For hydrogen and carbon atoms, TMS was used as the reference (σ(H) = 30.84 ppm[54] and σ(C) = 188.1 ppm[55]). For nitrogen, the references were NH_3 and nitromethane (σ(N) = 264.5 ppm[56] and σ(N) = -135.8 ppm,[57] respectively).

As shown in Table 4, results of calculations performed at KT3/cc-pCVTZ level of theory are close to the experimental values in thymine and 9-methyl adenine. Specially our theoretical values of $\delta(N_3)$ in thymine and $\delta(N_6)$ in 9-Me-adenine do reproduce experimental measurements quite well. All other results are within 10 %

Table 4 Shieldings and chemical shifts in 9-Methyl adenine and thymine with the KT3/cc-pCVTZ level of theory. All values are in ppm

	σ	δ^a	δ^b_{exp}	δ^c	δ^d_{exp}
9-Me-adenine					
N_1	14.69	249.81	236.10	-150.49	-144
N_3	20.40	244.10	226.10	-156.20	-157
N_6	182.21	82.29	81.10	-318.01	-297
C_2	36.92	151.18	152.35		
C_6	37.88	150.22	155.83		
H_2	23.62	7.22	8.14		
thymine					
N_1	119.54			-255.34	-236
N_3	88.81			-224.54	-224

[a]Values obtained using TMS as a reference for hydrogen and carbon, and NH_3 for nitrogen.
[b]Experimental values taken from Ref.[12](TMS was used as a reference for H and C, and NH_3 for N).
[c]Values obtained using nitromethane as a reference.
[d]Experimental values taken from Ref.[17](where the nitromethane was used as the reference for N).

of difference.

All shielding calculations were performed with the LDBS scheme mentioned above, at DFT(KT3/cc-pCVTZ/cc-pVTZ) level of theory. On the other hand, J-couplings were calculated without considering the LDBS scheme and using B3LYP/6-311G(2df, 2pd) level of theory, which is equivalent to B3LYP/cc-pVTZ level of theory that gave comparable results to the SOPPA method.

4.2 NMR Spectroscopic Parameters of AT and GC Pairs and layers of DNA base pairs

We shall analyse now the effect of piling up base pairs. The procedure we follow was explained in Section 2.

4.2.1 Shieldings

We start with the analysis of the shieldings of selected atoms that belong to the main part of the bonding structure of each base pair. In Tables 5 and 6 results of calculations of such shieldings are given for the same base pairs in different layers.

The experimental geometrical structures of base pairs and helical layers of base pairs were taken as they are in the 1BNA structure of the PDB data bank mentioned in Section 2. Geometrical structures of the monomers, together with base pairs of AT and GC were also theoretically optimized and so we are also able to compare results of shielding calculations using experimental geometries with that arising from theoreticaly optimized geometrical structures.

In Table 5 the values of shieldings and chemical shifts calculated with the above mentioned level of theory and geometries are shown. We only include the shielding of atoms that are located in the region close to HB, which highly feels the influence of the other pairs and also of the stacking. The theoretical chemical shifts for H_3 of thymine and H_6 of adenine are close to their experimental values. The same happens for carbons C_2. In the case of nitrogen atoms their theoretical chemical shifts are not close to the experimental values. The difference in these last cases are $\approx$ 10%, and are also in line with what was mentioned in the Section 3.

We only include the shielding of the nitrogen atoms that are involved in HB, *i.e.* $N_1\cdots H_3$-N_3 and N_6-$H_6\cdots O_4$. If the optimized structures are considered, only the shielding of donor nitrogens vary appreciable when the differences among monomers and dimers are considered. In the case of thymine, $\sigma(N_3)$ varies from 88.81 ppm (monomer) to 81.08 ppm (dimer); for adenine the values of $\sigma(N_6)$ are 181.78 ppm and 171.86 ppm, respectively. In this last monomer the behavior of $\sigma(N_1)$ is similar to that of an acceptor atom, so that it becomes more shielded after the pair was formed. Its shielding goes from 13.41 ppm to 28.95 ppm.

On the other side, two of the three hydrogen atoms that are considered, the H_6 of adenine and H_3 of thymine show large reduction of its shieldings: from 27.19 ppm to 22.43 ppm and from 24.89 to 17.06 ppm, respectively. The shielding of H_2 of adenine does not vary. This behavior can be expected due to such hydrogen does not belongs to an HB.

The deshielding behavior of H_6 and H_3 are such that the largest effect is observed in H_3 (its deshielding is of 31.46 %) being the deshielding of H_6 half of it (17.51 %). This means that the shielding of the hydrogen that belongs to the homonuclear bond $N_1\cdots H_3$-N_3 is more deshielded than the shielding of the hydrogen which belongs to an heteronuclear bond, N_6-$H_6\cdots O_4$.

Now we are able to state that the amount of the deshielding of the hydrogens that belong to HB is related with the strength of the hydrogen bonding.[4] As an example, the strength of the bond to which H_3 belongs, which is deshielded by 31.46 % is larger than that of the bond to which H_6 belongs, which is deshielded by 17.51 %.

We continues with the analysis of the shielding of carbons. In general, the variation of the shielding of C_2 of adenine and C_2 of thymine are very small. Still carbons C_6 of adenine and C_4 of thymine are located in special places of the molecule. They are close to the HB. Both carbons are deshielded though the carbon C_4 is more deshielded. The reason for this is the fact that C_6 is

Table 5 Magnetic shieldings and chemical shifts for the adenine-thymine pair (in ppm) calculated at KT3//cc-pCVTZ/cc-pVTZ level of theory

	adenine						thymine			
	N_6	N_1	C_6	C_2	H_6	H_2	N_3	C_2	C_4	H_3
Magnetic shielding										
Monomer with opt geometry[a]	181.78	13.41	37.90	36.35	27.19	23.38	88.81	42.35	29.75	24.89
Base pair with opt geometry[a]	171.86	28.95	35.57	37.30	22.43	23.13	81.08	41.20	23.99	17.06
Isolated AT pair[b]	174.87	31.77	35.30	38.04	24.83	23.16	85.91	37.58	26.34	17.36
ATT[c]	170.63	31.85	36.24	36.05	24.81	23.33	85.34	38.37	26.94	17.91
A**ATT**C[c]	170.00	31.82	36.35	36.45	25.07	23.58	85.44	38.51	27.31	18.20
Chemical shift										
Dimer with opt geometry	92.64		152.5	150,8	8.41		183.4	146.90	164.11	13.78
Isolated AT pair	89.63		152,8	150.06	6.01		178.59	150.52	161.76	13.48
ATT	93.87		151.86	152.05	6.03		179.16	149.73	161.16	12.93
Exp.[d]	82-84		157-158	152-156	7-8		156	154	169	13-14

[a]The optimized structures for each monomer and the AT pair.
[b]The central AT pair which is isolated of the sequences of three pairs (ATT) and five pairs (AATTC).
[c]The central AT pair inserted in the sequence of three and five pairs.
[d]Experimental values of chemical shifts taken from Ref.[58].

bonded to the nitrogen N_6, which is deshielded, and to N_1 which is more shielded. On the other hand the carbon C_4 is bonded to the nitrogen N_3, which is deshielded more than the N_6 of adenine.

Table 6 is equivalent to Table 5 though for the shieldings of guanine and cytosine. As was shown for adenine and thymine, the theoretical chemical shifts of hydrogens are closer to their experimental values than the chemical shifts of carbons and nitrogen are. This is especially the case for hydrogens in adenine. Again, the nitrogen chemical shifts obtained by calculations are $\approx$ 10% away of experimental values. The chemical shifts of the carbons bonded to oxygens are the more difficult to reproduce. The others are much better reproduced by the DFT level of theory used in this work.

For the pairs of guanine-cytosine we analysed in more detail the shielding of the four nitrogens that belongs to three hydrogen bonds, *i.e.* N_1-$H_1\cdots N_3$, N_2-$H_2\cdots O_2$ and $O_6\cdots H_4$-N_4. As happens in the case of adenine and thymine, those nitrogen atoms that are donor in a heteronuclear HB interaction will have a reduction of their shieldings, when the shieldings in the monomer and the pair are compared each other. The shielding of nitrogen N_2 of guanine varies from 186.92 ppm to 177.57 ppm; and for nitrogen N_4 of cytosine its shieldings vary from 172.72 ppm to 148.79 ppm, being both part of heteronuclear bondings. On the other hand the nitrogen N_1 of guanine varies from 98.31 ppm to 100.48 ppm and again its behavior is similar to that of a donor which belongs to a homonuclear interaction. In the case of acceptor atoms, the value of the shielding for N_3 of cytosine varies from 27.00 ppm to 45.63 ppm, following the typical behavior of similar atoms in the AT pair.

Turning now to the hydrogen atoms, the shieldings of three hydrogen atoms were analysed: H_1 and H_2 of guanine and H_4 of cytosine. They belong to the three HB that participate in the bonding among guanine and cytosine. This is the reason why all these hydrogens are deshielded. For H_1 the variation is of 24.87 %; for H_2 it is of 19.16 % and 27.60 % for H_4. The behavior of the shieldings in this pair is different of that of the AT, because the shieldings in homonuclear interactions have a large proportion of changes. Still, in the heteronuclear interactions like $O_6\cdots H_4$-N_4, the variation is even larger.

As happens for AT we can relate again the percentage of the deshielding of hydrogen atoms with the strength of the HB. Applying this criterium we can stablish a relation for all the three bondings, which contain the three hydrogens we are talking about. Such order is: N_2-$H_2\cdots O_2 <$ N_1-$H_1\cdots N_3 < O_6\cdots H_4$-$N_4$, which coincide with previous findings.[4]

Concerning carbon atoms, we can see that C_2 and C_6 that belongs to guanine, and C_2 and C_4 of cytosine, are located among the three centers in which the hydrogen bondings are produced, so that the highest electronic activity is in there. These four carbon atoms are deshielded when the pair is stablished, being the carbon C_6 of guanine and the carbon C_4 of cytosine the more influenced due to their proximity to the places where the large variations of shieldings do occur.

Let us analize now what happens to the systems that contain more than one pair of bases. Due to the fact that some pairs contain two HB and other contain three HB, as mentioned in Section 2, we have selected helical layers which are more rich in GC or AT pairs each.

Because of we are interested in using only one pair as a

Table 6 Magnetic shielding and chemical shift for guanine-cytosine pair (in ppm) calculated at KT3//cc-pCVTZ/cc-pVTZ level of theory

	Guanine						Cytosine				
	N_1	N_2	C_6	C_2	H_1	H_2	N_4	N_3	C_4	C_2	H_4
Magnetic shielding											
Monomer with opt geometry[a]	98.31	186.92	38.66	39.59	24.93	28.39	172.72	27.00	29.72	40.01	27.43
Dimer with opt geometry[a]	100.48	177.57	32.31	37.72	18.73	22.95	148.79	45.63	26.67	36.33	19.86
Isolated GC pair[b]	105.60	177.81	34.23	36.06	18.69	22.29	148.49	47.76	25.04	38.22	20.19
GCG[c]	102.66	168.63	34.19	34.68	18.71	22.25	147.91	48.64	25.58	38.97	20.83
C**GCG**A[c]	102.89	168.70	34.34	34.96	19.01	22.60	148.53	48.28	25.76	39.21	21.01
Chemical shift											
Dimer with opt geometry[a]	164.02	86.93	155.79	150.38	12.11	7.89	115,71	218.87	161,43	151,77	10.98
Isolated GC pair[b]	158.9	86.29	153.87	152.04	12.15	8.55	116.01	216.74	163.06	149.88	10.65
GCG	161.84	95.87	153.91	153.42	12.13	8.59	116.59	215.86	162.52	149.13	10.01
Exp.[d]	146-149	72-76	161	156	12-13.6	8-9	94-98	210	166-168	159	8.1-8.8

[a]Optimized structures for each monomer and dimer of the GC pair.
[b]The central GC pair which is isolated of the sequences of three (GCG) and five (CGCGA) pairs.
[c]The central GC pair inserted in the sequence of three and five pairs.
[d]Experimental values of chemical shifts, taken from Ref.[58]

probe of what is happening in a given fragment, we have chosen the central pair of CGCGA, numbered as 3, and the central pair of AATTC, numbered as 7. So, in each case, we studied the magnetic properties of the central pair in three different systems: a) when the central pair is isolated (meaning alone); b) when the central pair is in the center of the sequence of three pairs and c) when the central pair is located in the center of five pairs.

In Table 5 we show the values of the shieldings for the AT pair in the three different systems mentioned above: a) when AT is isolated (it corresponds to the pair 7), b) when AT is in the sequence of three pairs (ATT or pairs 678) and c) when AT is in the sequence of five pairs (AATTC or pairs 56789). One can see that the nitrogen N_6 of adenine is the most sensitive to the changes of the environment, from a) to b). Its shielding changes from 174.87 ppm to 170.63 ppm. Furthermore, when more pairs are added, above and below of the central pair, a very small change does appear.

In the same manner we observe that $\sigma(C_6)$ of adenine do increase, together with $\sigma(C_2)$ and $\sigma(C_4)$ of thymine when one consider more complex structures. This is mainly the case when one analyse the shieldings of the isolated pairs and compare them with the shieldings in the ATT fragment. The difference of the shieldings of the isolate AT pair with that of the same pair in the middle of the AATTC fragment is even larger.

On the other hand the behavior of $\sigma(C_2)$ of adenine is different. It changes from 38.04 ppm to 36.05 ppm when going from the isolated AT to the AT pair located in the middle of ATT; and then, instead of continuing diminishing when considered in the middle of AATTC its shielding goes up. In the case of hydrogen atoms, only H_3 of thymine is more sensitive to the environment. This is clear for the shieldings in the isolated pair and the same pair in the AATTC sequence.

The shieldings of our selected atoms of the GC pair are given in Table 6. As was just done for the AT pair, we shall analyse the variation of its shieldings in the isolated system (which correspond to the pair 3), the sequence of three pairs (GCG or pairs 234) and the sequence of five pairs (CGCGA or pairs 12345).

In general, the shielding of nitrogen atoms show a difference when one goes from the isolated GC pair to the pair in the middle of the sequence of three pairs, GCG. $\sigma(N_1)$ and $\sigma(N_2)$ of guanine have the largest differences: from 105.60 ppm to 102.66 ppm, and from 177.81 ppm to 168.63 ppm, respectively.

As happens in the helical layers that are richer in AT pairs, in the GC case the value of the shieldings does not vary much from GCG to CGCGA. On the other hand there is a difference with previous AT pairs because the difference of shieldings that appears among the sequence of three and five pairs is opposite of what happens in previous AT pairs.

We should stress here the fact that there are some atoms that are more sensitive to the piling up. In the case of carbons, the atoms C_2 in guanine and C_2 in cytosine are the most sensitive, even though the first one is more deshielded. This is due to the fact that C_2 in cytosine is located between the nitrogens N_1 and N_2, and they are more affected when they belong to the fragment GCG.

In the case of hydrogens, H_1 and H_2 of guanine and H_4 of cytosine show a tendency to increase. The largest variation for their shieldings occurs among the isolated pair and the fragment of five pairs.

As a summary, in Table 7 we give the variations of the values of shieldings of atoms that belongs to some of the base pairs. The sequence that is considered in this Table

is: Isolated → three base pairs → five base pairs. They show some similarities that must be stressed.

Table 7 Pattern of variations of the values of shieldings for atoms that belong to some of the base pairs

Sequence	1 → 3 → 5	1 → 3 → 5
Atom\Base	Thymine (shieldings) (ppm)	Cytosine (shieldings, ppm)
C_2	37.58 → 38.37 → 38.51	38.22 → 38.97 → 39.21
C_4	26.34 → 26.94 → 27.31	25.04 → 25.58 → 25.76
H_3; H_4	17.36 → 17.91 → 18.20	20.19 → 20.83 → 21.01
Atom\Base	Thymine (shieldings, ppm)	Guanine (shieldings, ppm)
H_3; H_1	17.36 → 17.91 → 18.20	18.69 → 18.71 → 19.01
Atom\Base	Adenine (shieldings, ppm)	Guanine (shieldings, ppm)
H_6; H_2	24.83 → 24.81 → 25.07	22.29 → 22.25 → 22.60
C_6; C_2	35.30 → 36.24 → 36.35	36.06 → 34.68 → 34.96
N_6; N_2	174.87→ 170.63 → 170.00	177.81 → 168.63 → 168.70

It is observed that equivalent atoms in equivalent bases have similar values of shieldings, *e.g.* the carbons C_2 and C_4 in thymine and cytosine, respectively; and hydrogens H_6 and H_2 in adenine and guanine, respectively. They follow the same pattern and its magnitudes are quite similar.

The shieldings of the nitrogen atoms that are donors in HBs, like the atoms N_2 in guanine and N_6 in adenine, vary around 4% to 5% when its values are taken from calculations of isolated GC or AT dimers, or taken from calculations of three layers of pairs. If these nitrogen shieldings are calculated in three to five layers of dimers, we found that its variation is quite small. So it seems that the shielding of those nitrogen atoms are more influenced by the stacking than by the cooperative effects within the helical layers of DNA molecules. A similar behavior is found for carbon atoms that are bonded to the just mentioned nitrogen atoms.

4.2.2 J-couplings

We now turn our analysis to the four electronic mechanisms that contribute to the indirect NMR J-couplings. They are: Fermi-contact, FC; Spin-Dipolar, SD; Paramagnetic spin-orbit, PSO and Diamagnetic spin-orbit, DSO. We do it in base pairs whose geometrical structures were either theoretically optimized, or taken as such from that layers of DNA base pairs we are interested in. In the last case we considered three possibilities, in the same manner as it was done for shieldings: isolated, in the middle of three base pairs and in the middle of five base pairs. For this spectroscopic parameter we have not studied the effect of pairing; meaning, how it changes when one consider first the monomers and then the pairs. We were only interested in the effect of piling up.

In Tables 8 and 9 we show results of calculations at B3LYP/6-311G(2df,2pd) level of theory for AT and GC pairs, respectively. This scheme is similar to that used by Marek and coauthors-[12] As observed in those Tables, our results are close to the experimental values.

Table 8 Contributions to J-couplings (in Hz) for adenine-thymine pair at B3LYP/6-311G(2df,2pd) level of theory

		FC	SD	PSO	DSO	Total	Exp.[a]
Optimized	$J(N_6\text{-}H_6)$	-90.07	-0.14	-1.51	-0.42	-92.14	
	$J(N_1\text{-}C_2)$	-4.50	-0.41	4.90	-0.13	-0.14	
	$J(N_1\text{-}N_3)$	-4.71	-0.06	0.03	-0.01	-4.75	
	$J(N_3\text{-}C_4)$	-13.44	-0.08	3.18	-0.17	-10.51	
	$J(N_3\text{-}H_3)$	-80.67	-0.06	-0.91	-0.60	-82.24	
Isolated	$J(N_6\text{-}H_6)$	-90.70	-0.22	-1.91	-0.39	-93.22	
	$J(N_1\text{-}C_2)$	-6.28	-0.39	4.62	-0.13	-2.18	
	$J(N_1\text{-}N_3)$	-4.94	-0.04	0.01	-0.01	-4.98	
	$J(N_3\text{-}C_4)$	-14.48	-0.08	3.07	-0.17	-11.66	
	$J(N_3\text{-}H_3)$	-90.94	-0.18	-0.81	-0.66	-92.59	
ATT	$J(N_6\text{-}H_6)$	-90.88	-0.24	-1.73	-0.53	-93.38	
	$J(N_1\text{-}C_2)$	-5.70	-0.41	4.66	-0.17	-1.62	
	$J(N_1\text{-}N_3)$	-4.88	-0.04	0.03	-0.03	-4.92	
	$J(N_3\text{-}C_4)$	-14.49	-0.08	3.10	-0.20	-11.67	
	$J(N_3\text{-}H_3)$	-90.46	-0.18	-0.65	-0.81	-92.10	
AATTC	$J(N_6\text{-}H_6)$	-90.74	-0.24	-1.70	-0.55	-93.23	88
	$J(N_1\text{-}C_2)$	-5.75	-0.41	4.67	-0.17	-1.66	
	$J(N_1\text{-}N_3)$	-4.88	-0.04	0.03	-0.03	-4.92	
	$J(N_3\text{-}C_4)$	-14.53	-0.08	3.10	-0.21	-11.72	10.7[b]
	$J(N_3\text{-}H_3)$	-90.48	-0.18	-0.62	-0.83	-92.11	91[b]

[a] Experimental values, taken from Ref.[58].
[b] Experimental values that correspond to uracil.

In most of our cases the main mechanism that contribute to J-couplings is the FC. The PSO mechanism is very important for $J(N_1\text{-}C_2)$ and $J(N_3\text{-}C_4)$ in the AT pair.

It is interesting to see that the value of nitrogen-nitrogen, donor-acceptor couplings, *i.e.* $J(N_1\text{-}N_3)$ of both, AT and GC, are close each other: -4.2 Hz and -4.9 Hz, respectively. They do not depend on the piling up of base pairs.

This last behavior is observed for all J-couplings, but still there are some new information which should be mentioned. The J-coupling $J(N_3\text{-}H_3)$ of thymine is reduced a little bit when one compare its value in an isolated pair with its value in the layers of three or five pairs.

On the other hand the $J(N_6\text{-}H_6)$ coupling in adenine increase its value smoothly when one goes from the isolated base pair to the stack of three and five layers of base pairs.

Considering the behavior of J-couplings for GC pairs we can see that there is a similar pattern in these pairs. For $J(N_1\text{-}H_1)$ and $J(N_4\text{-}H_4)$ we found patterns that are similar to those of the AT pair, when one consider the isolated, and then the three and five pairs of dimers. On the other hand the coupling $J(N_2\text{-}H_2)$ increase smoothly its value when considered first the isolated pair and the fragment of three pairs. Then it does not increase any longer. Lastly $J(N_1\text{-}N_3)$ and $J(C_6\text{-}N_1)$ also increase when

Table 9 J-couplings (in Hz) for guanine-cytosine pair at B3LYP/6-311G(2df,2pd) level of theory

		FC	SD	PSO	DSO	Total	Exp.[a]
Optimized	$J(C_6\text{-}N_1)$	-12.91	-0.17	2.88	-0.15	-10.35	
	$J(N_1\text{-}H_1)$	-80.27	-0.03	-1.21	-0.60	-82.12	
	$J(N_1\text{-}N_3)$	-3.53	-0.04	0.03	-0.01	-3.56	
	$J(N_2\text{-}H_2)$	-86.77	-0.13	-1.53	-0.42	-88.86	
	$J(N_4\text{-}H_4)$	-85.68	-0.13	-1.05	-0.42	-87.29	
Isolated	$J(C_6\text{-}N_1)$	-17.02	-0.15	3.02	-0.17	-14.32	
	$J(N_1\text{-}H_1)$	-80.06	-0.10	-1.15	-0.67	-81.98	
	$J(N_1\text{-}N_3)$	-4.12	-0.04	0.04	-0.01	-4.13	
	$J(N_2\text{-}H_2)$	-88.54	-0.15	-1.32	-0.46	-90.47	
	$J(N_4\text{-}H_4)$	-90.04	-0.22	-0.91	-0.45	-91.62	
GCG	$J(C_6\text{-}N_1)$	-17.17	-0.14	3.04	-0.20	-14.47	
	$J(N_1\text{-}H_1)$	-80.20	-0.11	0.90	-0.83	-82.04	
	$J(N_1\text{-}N_3)$	-4.22	-0.04	0.04	-0.01	-4.23	
	$J(N_2\text{-}H_2)$	-88.84	-0.17	-1.08	-0.59	-90.68	
	$J(N_4\text{-}H_4)$	-90.04	-0.22	-0.80	-0.58	-91.64	
C**GCG**A	$J(C_6\text{-}N_1)$	-17.24	-0.14	3.07	-0.21	-14.52	7.5
	$J(N_1\text{-}H_1)$	-80.15	-0.11	-0.88	-0.84	-81.98	90
	$J(N_1\text{-}N_3)$	-4.22	-0.04	0.04	-0.03	-4.25	5.5[b]
	$J(N_2\text{-}H_2)$	-88.81	-0.18	-1.07	-0.62	-90.68	91
	$J(N_4\text{-}H_4)$	-90.01	-0.22	-0.77	-0.59	-91.59	86

[a] Experimental values taken from Ref.[58].
[b] Experimental value taken from Ref.[9].

going from isolated pairs to small agregate of base pairs.

The one-bond $J(N_3\text{-}H_3)$ coupling of the HB in the AT pair vary from -92.6 Hz when it is isolated, to -92.1 Hz when the pair belong to a layer. This is not the case for the equivalent one-bond coupling in the GC pair.

4.2.3 Dispersion effects on σ and J-couplings

In order to know how important are dispersion effects on both, σ and J NMR spectroscopic parameters, we performed some calculations at B97 level of approach,[59] and its equivalent dispersion including functional *i. e.* B97-D.[60] In Tables S16-S18 of the Supporting Information, we show results of calculations for the fragments richer in GC pairs. In Table 10 a comparison of the percentage of variations of the same shieldings of Table 6 calculated at KT3 and B97-D level of theory are shown. They are of the same order of magnitude and follows the same pattern. A similar behavior was found for J-couplings (see Table S18 of SI). Then dispersion effects do not modify our main findings.

Table 10 Percentage of change of magnetic shieldings for guanine-cytosine pair (in %) calculated at KT3 and B97-D level of theory

	Guanine						Cytosine				
	N_1	N_2	C_6	C_2	H_1	H_2	N_4	N_3	C_4	C_2	H_4
KT3	-2.78	-5.16	=	-3.83	=	=	-0.39	1.84	2,16	1.96	3.17
B97-D	-3.41	-5.86	=	-6.49	=	=	-0.71	2.28	2.45	2.00	3.15

5 Conclusions

During the last few years we have been studying the influence of hydrogen bonds on magnetic properties, and also how long can the magnetic effects on NMR spectroscopic parameters be transmitted. Then we recently turned to the studies of the influence of pi-stacking on magnetic properties of atoms that belongs to base pairs in sequences of layers of base pairs of DNA. Those parameters are quite sensitive to the electronic effects of the environment and, at the same time, they are usually of a local nature.

In this work we have analized the transmission of magnetic interactions in layers of DNA molecules which are richer in either, AT pairs or GC pairs. We have found that there are some nuclei belonging to those layers whose magnetic properties may be used as a reliable probe of the likely intermolecular magnetic interactions. They have among its sources both, the hydrogen bonds and the stacking interactions, together with the geometrical disposition of all base pairs in the layers of trimers and pentamers. We analysed how important is the effect of the piling up of several base pairs above and below a central pair, taken it as the witness and whose atoms are used as receptors of the magnetic influence of the environment. Those interactions modify their NMR spectroscopic parameters in a small but not vanishingly small amount. We also found that dispersion effects do not change such pattern of variations.

In all cases we found that magnetic shieldings are more sensitive to the changes in the neighborhood of the central base pair, than J-couplings. A clear, though still preliminary pattern for shieldings, has appeared from our calculations: i) equivalent atoms in any of the similar monomers (say thymine and cytosine) do have equivalent values of the shieldings when they are paired (AT and GC, respectively), and the pattern of variations due to pi-stacking is also similar; so that the influence of pi-stacking on equivalent atoms is similar, ii) the shielding of hydrogens in HBs are more sensitive to the piling up than the non-hydrogen atoms, meaning that they vary a percentage that may be of the order of 5% when going from a sequence of one to five layers of base pairs.

An interesting finding has to do with the importance of the influence of stacking on NMR magnetic shieldings of nitrogens that are donors in HBs, and the carbons that are bonded to them. We found that the shielding of those atoms vary among 2% to 5% if they are first considered in the isolated pair and then, belonging to some of the trimers and pentamers of base pairs. If we compare the shieldings of those nitrogen atoms when they belong to some of both sequences of helical layers (containing three or five layers) we do not find such a difference; this is now very small. This supports the hypothesis

that pi-stacking do affect the shielding of nitrogens that are donor of HBs and the shielding of carbons bonded to them.

Another finding of our studies was the fact that one must use larger basis set than cc-pVTZ if one wants to obtain reliable NMR magnetic shieldings of layers of DNA base pairs.

Conflicts of Interest There are no conflicts of interest to declare.

Acknowledgements

This research has been partially supported by the Argentinian Research Council on Science and Technology, CONICET (Grant PIP 112-20130100361), and by the Agency for Promotion of Science and Technology of Argentina, FONCYT (Grant PICT2012-1214).

References

1 J. Rezáč and P. Hobza, *Chem.-A Eur. J.*, 2007, **13**, 2983–2989.
2 L. Guillaumes, S. Simon and C. Fonseca Guerra, *ChemistryOpen*, 2015, **4**, 318–327.
3 J. Poater, M. Swart, F. M. Bickelhaupt and C. Fonseca Guerra, *Org. Biomol. Chem.*, 2014, **12**, 4691–4700.
4 H. Szatylowicz and N. Sadlej-Sosnowska, *J. Chem. Inf. Model.*, 2010, **50**, 2151–2161.
5 J. Černý, M. Kabelác and P. Hobza, *J. Am. Chem. Soc.*, 2008, **130**, 16055–16059.
6 C. Fonseca Guerra, F. M. Bickelhaupt, J. G. Snijders and E. J. Baerends, *Chem. Eur. J.*, 1999, **5**, 3581–3594.
7 F. Kilchherr, C. Wachauf, B. Pelz, M. Rief, M. Zacharias and H. Dietz, *Science*, 2016, **353**, aaf5508.
8 J. Poater, M. Swart, C. Fonseca Guerra and F. M. Bickelhaupt, *Chem. Comm.*, 2011, **47**, 7326–7328.
9 B. Fürtig, C. Richter, J. Wöhnert and H. Schwalbe, *Chembiochem*, 2003, **4**, 936–962.
10 N. Juranic, P. K. Ilich and S. Macura, *J. Am. Chem. Soc.*, 1995, **117**, 405–410.
11 N. Juranic, V. A. Likic, F. G. Prendergast and S. Macura, *J. Am. Chem. Soc.*, 1996, **118**, 7859–7860.
12 R. Marek, A. Křístková, K. Maliňáková, J. Toušek, J. Marek, M. Hocek, O. L. Malkina and V. G. Malkin, *J. Phys. Chem. A*, 2010, **114**, 6689–6700.
13 R. Fiala, M. L. Munzarová and V. Sklenář, *J. Biomolec. NMR*, 2004, **29**, 477–490.
14 J. M. Fonville, M. Swart, Z. Vokáčová, V. Sychrovská, J. E. Šponer, J. Šponer and S. S. Wijmenga, *Chem.-A Eur. J.*, 2012, **18**, 12372–12387.
15 A. J. Dingley, J. E. Masse, R. D. Peterson, M. Barfield, J. Feigon and S. Grzesiek, *J. Am. Chem. Soc.*, 1999, **121**, 6019–6027.
16 M. Barfield, A. J. Dingley, J. Feigon and S. Grzesiek, *J. Am. Chem. Soc.*, 2001, **123**, 4014–4022.
17 J. Z. Hu, J. C. Facelli, D. W. Alderman, R. J. Pugmire and D. M. Grant, *J. Am. Chem. Soc.*, 1998, **120**, 9863–9869.
18 A. Asensio, N. Kobko and J. J. Dannenberg, *J. Phys. Chem. A*, 2003, **107**, 6441–6443.
19 T. van Mourik and A. J. Dingley, *J. Phys. Chem. A*, 2007, **111**, 11350–11358.
20 K. Sutter, G. A. Aucar and J. Autschbach, *Chem.-A Eur. J.*, 2015, **21**, 18138–18155.
21 N. Zarycz, G. A. Aucar and C. O. Della Védova, *J. Phys. Chem. A*, 2010, **114**, 7162–7172.
22 A. D. Becke, *J. Chem. Phys.*, 1993, **98**, 5648–5652.
23 C. Lee, W. Yang and R. G. Parr, *Phys. Rev. B*, 1988, **37**, 785–789.
24 E. S. Nielsen, P. Jorgensen and J. Oddershede, *J. Chem. Phys.*, 1980, **73**, 6238–6246.
25 M. J. Packer, E. K. Dalskov, T. Enevoldsen, H. J. R. A. Jensen and J. Oddershede, *J. Chem. Phys.*, 1996, **105**, 5886–5900.
26 K. L. Bak, H. Koch, J. Oddershede, O. Christiansen and S. P. Sauer, *J. Chem. Phys.*, 2000, **112**, 4173–4185.
27 P. F. Provasi, G. A. Aucar, M. Sanchez, I. Alkorta, J. Elguero and S. P. Sauer, *J. Phys. Chem. A*, 2005, **109**, 6555–6564.
28 P. F. Provasi, G. A. Aucar and S. P. A. Sauer, *J. Phys. Chem. A*, 2004, **108**, 5393–5398.
29 A. D. Becke, *J. Chem. Phys.*, 1993, **98**, 1372–1377.
30 T. W. Keal and D. J. Tozer, *J. Chem. Phys.*, 2003, **119**, 3015–3024.
31 T. W. Keal and D. J. Tozer, *J. Chem. Phys.*, 2004, **121**, 5654–5660.
32 H. Kjaer, S. P. Sauer and J. Kongsted, *J. Chem. Phys.*, 2010, **133**, 144106–144119.
33 J. Gauss, *J. Chem. Phys.*, 1993, **99**, 3629–3643.
34 A. A. Auer, J. Gauss and J. F. Stanton, *J. Chem. Phys.*, 2003, **118**, 10407–10417.
35 T. Helgaker, M. Jaszuński and M. Pecul, *Chem. Rev.*, 1999, **99**, 293–352.
36 J. Vaara, *Phys. Chem. Chem. Phys.*, 2007, **9**, 5399–5418.
37 T. Helgaker, M. Jaszuński and K. Ruud, *Prog. in NMR Spectroscopy*, 2008, **53**, 249–268.
38 A. Perera, *Molec. Phys.*, 2010, **108**, 3017–3025.
39 J. Kongsted, K. Aidas, K. V. Mikkelsen and S. P. Sauer, *J. Chem. Theor. Comput.*, 2008, **4**, 267–277.
40 D. B. Chesnut and K. D. Moore, *J. Comput. Chem.*, 1989, **10**, 648–659.
41 D. B. Chesnut, B. E. Rusilosky, K. D. Moore and D. A. Egolf, *J. Comput. Chem.*, 1993, **14**, 1364–1375.
42 G. A. DiLabio, *J. Phys. Chem. A*, 1999, **103**, 11414–11424.
43 W. J. Hehre, R. Ditchfield and J. A. Pople, *J. Chem. Phys.*, 1972, **56**, 2257–2261.
44 M. J. Frisch, J. A. Pople and J. S. Binkley, *J. Chem. Phys.*, 1984, **80**, 3265–3269.
45 T. H. Dunning Jr, *J. Chem. Phys.*, 1989, **90**, 1007–1023.
46 D. E. Woon and T. H. Dunning Jr, *J. Chem. Phys.*, 1993, **98**, 1358–1371.
47 R. A. Kendall, T. H. Dunning Jr and R. J. Harrison, *J. Chem. Phys.*, 1992, **96**, 6796–6806.
48 D. E. Woon and T. H. Dunning Jr, *J. Chem. Phys.*, 1995, **103**, 4572–4585.
49 R. Ditchfield, *J. Chem. Phys.*, 1972, **56**, 5688–5691.
50 K. Wolinski, J. F. Hinton and P. Pulay, *J. Am. Chem. Soc.*, 1990, **112**, 8251–8260.
51 T. Helgaker, P. J. Wilson, R. D. Amos and N. C. Handy, *J. Chem. Phys.*, 2000, **113**, 2983–2989.
52 Aidas, K.; Angeli, C.; Bak, K. L.; Bakken, V.; Bast, R.; Boman, L.; Christiansen, O.; Cimiraglia, R.; Coriani, S.; Dahle, P.; Dalskov, E. K.; Ekström, U.; Enevoldsen, T.; Eriksen, J. J.; Ettenhuber, P.; Fernández, B.; Ferrighi, L.; Fliegl, H.; Frediani, L.; Hald, K.; Halkier, A.; Hättig, C.; Heiberg, H.; Helgaker, T.; Hennum, A. C.; Hettema, H.; Hjertenæs, E.; Høst, S.; Høyvik, I.-M.; Iozzi, M. F.; Jansik, B.; Jensen, H. J. Aa.; Jonsson, D.; Jørgensen, P.; Kauczor, J.; Kirpekar, S.; Kjærgaard, T.; Klopper, W.; Knecht, S.; Kobayashi, R.; Koch, H.; Kongsted, J.; Krapp, A.; Kristensen, K.; Ligabue, A.; Lutnæs, O. B.; Melo, J. I.; Mikkelsen, K. V.; Myhre, R. H.; Neiss, C.; , Nielsen, C. B.; Norman, P.; Olsen, J.; Olsen, J. M. H.; Osted, A.; Packer, M. J.; Pawlowski, F.; Pedersen, T. B.; Provasi, P. F.; Reine, S.; Rinkevicius, Z.; Ruden, T. A.; Ruud, K.; Rybkin, V.; Salek, P.; Samson, C. C. M.; Sánchez de Merás, A.; Saue, T.; Sauer, S. P. A.; Schimmelpfennig, B.; Sneskov, K.; Steinda, A. H.; Sylvester-Hvid, K. O.; Taylor, P. R.; Teale, A. M.; Tellgren, E. I.; Tew, D. P.; Thorvaldsen, A. J.; Thøgersen, L.; Vahtras, O.; Watson, M. A.; Wilson, D.

J. D.; Ziolkowski, M.; Ågren, H. , The Dalton quantum chemistry program system, WIREs Comput. Mol. Sci. 2014, 4:269–284 (doi: 10.1002/wcms.1172).
53 Y. Y. Rusakov and L. B. Krivdin, *Russ. Chem. Rev.*, 2013, **82**, 99–130.
54 I. Alkorta and J. Elguero, *J. Struct. Chem.*, 1998, **9**, 187–202.
55 A. K. Jameson and C. J. Jameson, *Chem. Phys. Lett.*, 1987, **134**, 461–466.
56 J. Gauss and J. F. Stanton, *J. Chem. Phys.*, 1995, **103**, 3561–3577.
57 C. J. Jameson and J. Mason, *Multinuclear NMR*, Plenum, 1987, p. 56.
58 S. S. Wijmenga and B. N. M. van Buuren, *Prog. Nucl. Magn. Reson. Spectrosc.*, 1998, **32**, 287–387.
59 A. D. Becke, *J. Chem. Phys.*, 1997, **107**, 8554–8560.
60 S. Grimme, *J. Comput. Chem.*, 2006, **27**, 1787–1799.

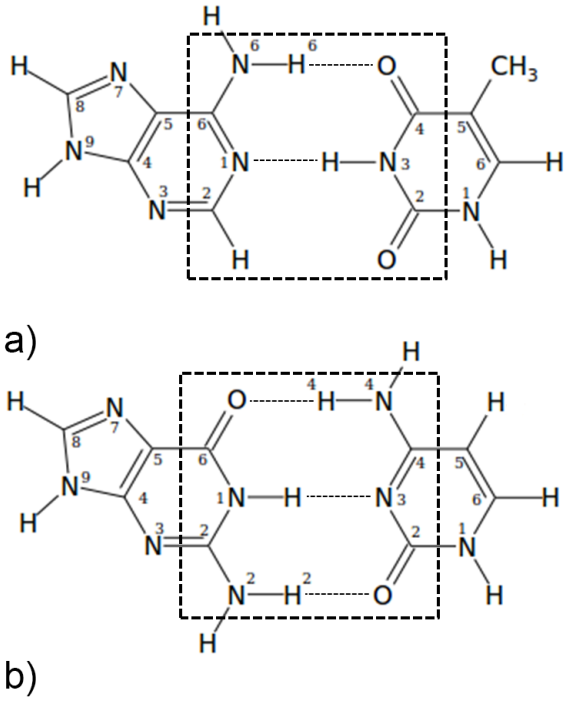

Fig. 1 Local dense basis set scheme of Watson-Crick DNA base pairs a) Adenine-Thymine (AT) and b) Guanine-Cytosine (GC).

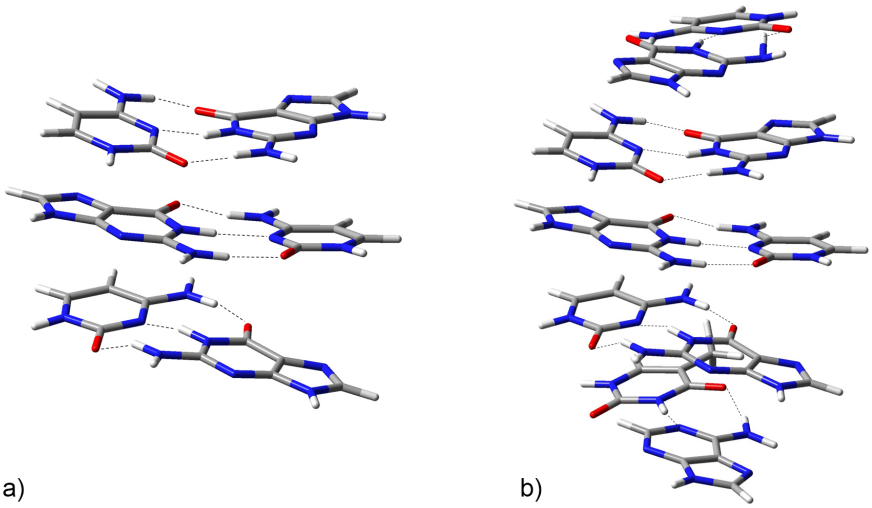

Fig. 2 a) Sequence of three stacked base pairs, GCG and b) Sequence of five stacked base pairs, CGCGA. All these helical layers were taken from crystallographic data without further geometric optimization. Only the position of the added hydrogen atoms were optimized